PROCEEDINGS OF SCIENCE

Measurement of Higgs boson production and properties

Matthias Saimpert, on behalf of the ATLAS and CMS collaborations[a,*]

[a] *IRFU, CEA, Université Paris-Saclay, Gif-sur-Yvette, France*

E-mail: matthias.saimpert@cea.fr

Thirteen years after its discovery, the Higgs boson remains at the centre of the LHC physics programme. Precision measurements of its production and decay provide unique tests of the Standard Model (SM) and sensitivity to possible new physics. The ATLAS and CMS experiments have collected unprecedented datasets at centre-of-mass energies of 13 and 13.6 TeV, enabling both detailed Run 2 "legacy" studies and first measurements with Run 3 data. The analyses cover a broad range of topics. This proceeding summarizes the latest ATLAS and CMS results on Higgs boson production and properties measurements, providing stringent tests of the Standard Model.

The Thirteenth Annual Large Hadron Collider Physics (LHCP2025)
5-9 May 2025
Taipei, Taiwan

*Speaker

https://pos.sissa.it/

PoS(LHCP2025)134

1. ATLAS and CMS datasets

During Run 2 (2015-2018), both ATLAS [1] and CMS [2] experiments recorded about 140 fb^{-1} of proton-proton collision data at $\sqrt{s}$ = 13 TeV, corresponding to nearly 8 million Higgs bosons produced per experiment. Run 3 (2022–2025) is expected to deliver about twice this luminosity at $\sqrt{s}$ = 13.6 TeV, with around 180 fb^{-1} of data already collected until 2024 (see Figure 1, left). The experiments achieved excellent object performance through high-efficiency detector operations and extensive calibrations (see Figure 1, right), enabling analyses with high precision.

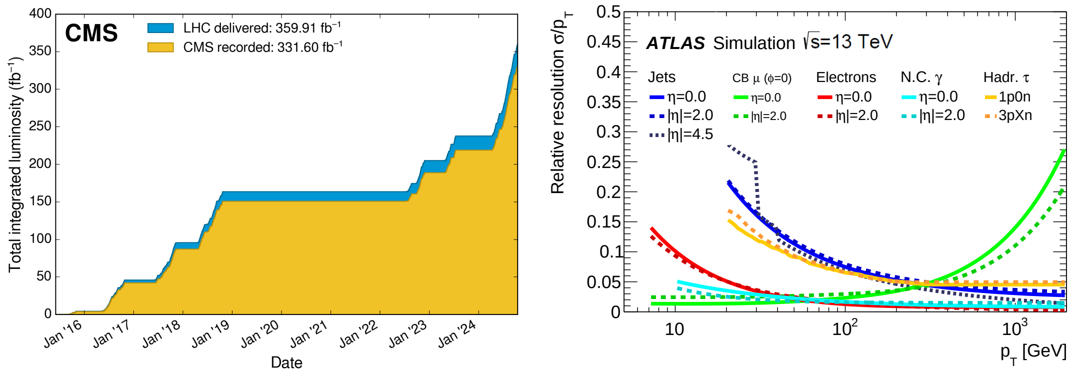

Figure 1: (left) Integrated luminosity versus time delivered by the LHC and recorded by the CMS experiment during Run 2 and Run 3 [3] and (right) relative resolutions of some typical objects used in ATLAS Run 2 analyses versus with the p_T of the object in question [4].

2. Early Run 3 results

One of the first results in the Higgs boson sector with Run 3 data is in the $H \to ZZ^* \to 4\ell$ channel. ATLAS reported inclusive and differential fiducial cross sections with 2022–2023 data (see Figure 2, left) [5], consistent with SM expectations, and set limits on effective field theory (EFT) operators. CMS performed a similar measurement with 2022 data, also finding good agreement (see Figure 2, right) [6]. Both collaborations have also released early $H \to \gamma\gamma$ cross-section results [7, 8], again in good agreement with the SM. These analyses demonstrate readiness for precision Higgs boson measurements with the Run 3 dataset.

3. Higgs width and mass (Run 2)

The intrinsic Higgs boson width, $\Gamma_H^{SM} \approx 4.1$ MeV, is too small to be resolved directly. ATLAS and CMS therefore exploit the on-shell to off-shell production ratio of both $H \to ZZ$ and $H \to WW$ decays. From Run 2 data, ATLAS measured $\Gamma_H = 4.3^{+2.7}_{-1.9}$ MeV [9] and CMS $3.0^{+2.0}_{-1.5}$ MeV [10], consistent with the SM (see Figure 3). To achieve this result, ATLAS introduced neural simulation-based inference (NSBI) to improve sensitivity in the 4ℓ channel. ATLAS also released the first Run 2 off-shell width result using $H^* \to WW$, setting an upper limit of 13.1 MeV at 95% CL [11] using this channel.

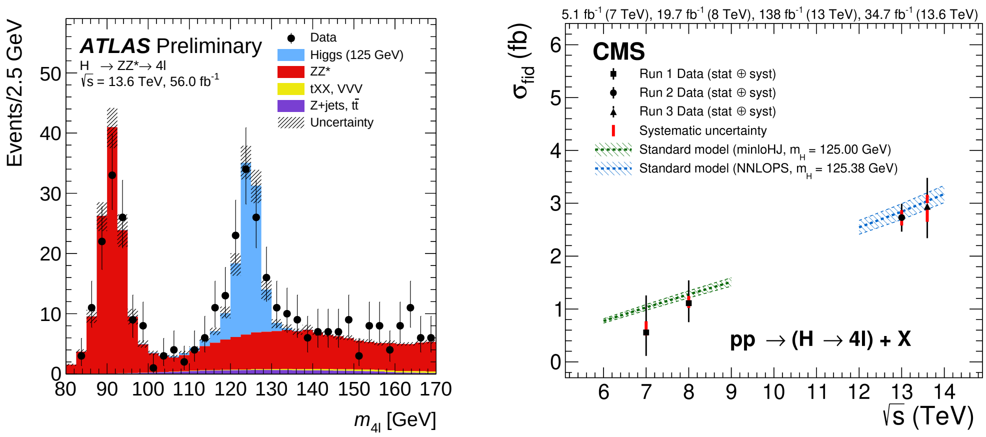

Figure 2: (left) Observed and expected (pre-fit) inclusive four-lepton invariant mass distribution measured by ATLAS in a partial Run 3 dataset [5]. (right) Measured inclusive fiducial $H \to ZZ^* \to 4\ell$ cross section as a function of the center-of-mass energy as measured by CMS [6].

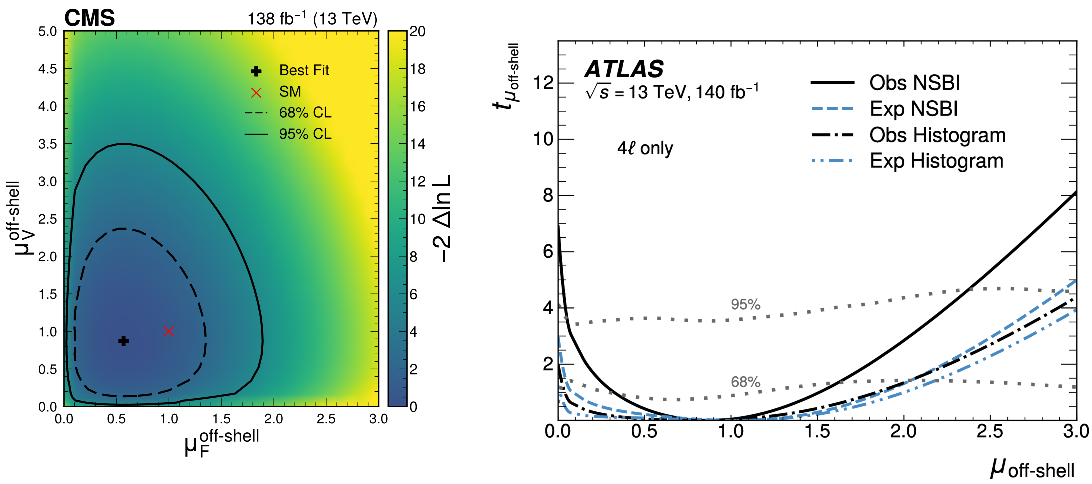

Figure 3: (left) Observed 2D profile likelihood projection of the off-shell signal strength parameters from the fit to the combined off-shell $H \to ZZ^* \to 4\ell$ and $2\ell 2\nu$ channels in CMS [10]. (right) Values of the test statistic $t_{\mu_{\text{off-shell}}}$ assuming a single parameter of interest $\mu_{\text{off-shell}}$ obtained with an Asimov dataset (expected, dashed blue) and with data (observed, solid black) in the ATLAS $H^* \to ZZ \to 4\ell$ decay channel [9]. The values from the histogram-based analysis are added in dash-dotted lines for comparison.

The Higgs boson mass is a free parameter in the Standard Model. It is measured most precisely in the $H \to \gamma\gamma$ and $H \to 4\ell$ channels. Using Run 1 and Run 2 data combined, ATLAS measured $m_{\text{H}} = 125.11 \pm 0.11$ GeV [12, 13], while CMS obtained $m_{\text{H}} = 125.08 \pm 0.12$ GeV [10, 14] (see Figure 4). Both experiments are consistent and achieve sub-per-mille precision (< 0.1‰). The final CMS analysis in the $H \to \gamma\gamma$ channel is still in preparation.

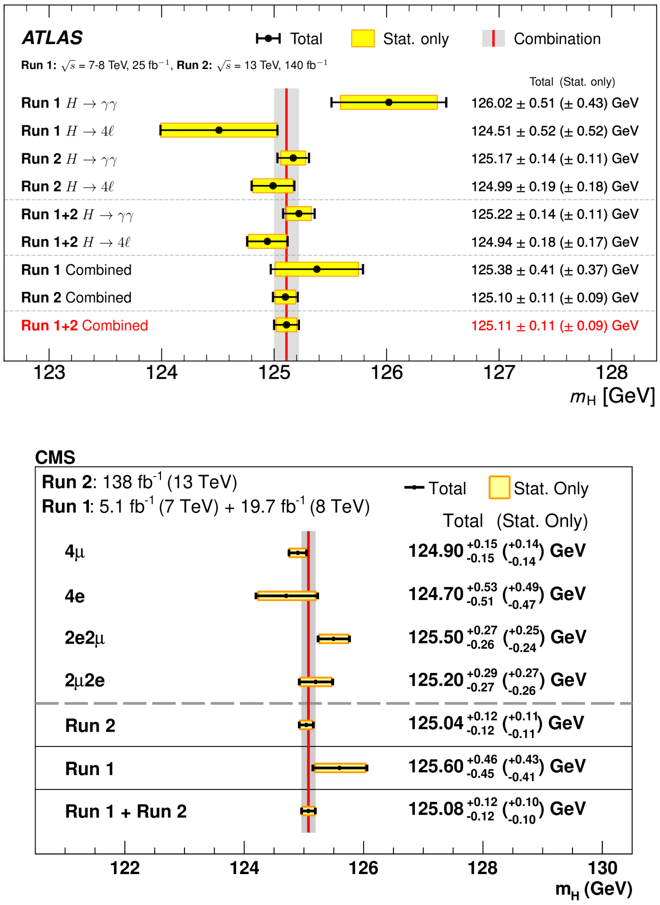

Figure 4: Summary of Higgs boson mass measurements performed by (top) ATLAS in the $H \to \gamma\gamma$ and $H \to 4\ell$ channels [12, 13] and (bottom) by CMS in the $H \to 4\ell$ channels [10].

4. Combined Higgs results (Run 2)

CMS has recently performed its most comprehensive combination to date [15], including 16 analyses across seven decay channels, interpreted in the simplified template cross-section (STXS) framework (see Figure 5) [16]. The inclusive signal strength was found to be $\mu = 1.014^{+0.055}_{-0.053}$, with precision ranging from 7% (gluon-gluon fusion) to 39% (tH) for production and from 8% ($H \to \gamma\gamma$) to 39% ($H \to Z\gamma$) for decays. The results are in excellent agreement with the SM. Constraints were also placed on the Higgs self-coupling, $\kappa_\alpha \in [-3.3, 9.6]$ at 95% CL, and on 43 operators from the Standard Model effective field theory (SMEFT), with good overall compatibility with the SM. The most comprehensive ATLAS combination to date remains the one published in Nature in 2022 [17].

5. Higgs–top sector (Run 2)

The associated production of a Higgs boson with top quarks provides a direct handle on the top Yukawa coupling. CMS has performed differential measurements of $t\bar{t}H$ events in multilepton final states [18], where the Higgs decays predominantly into WW^* or $\tau\tau$. The results are consistent

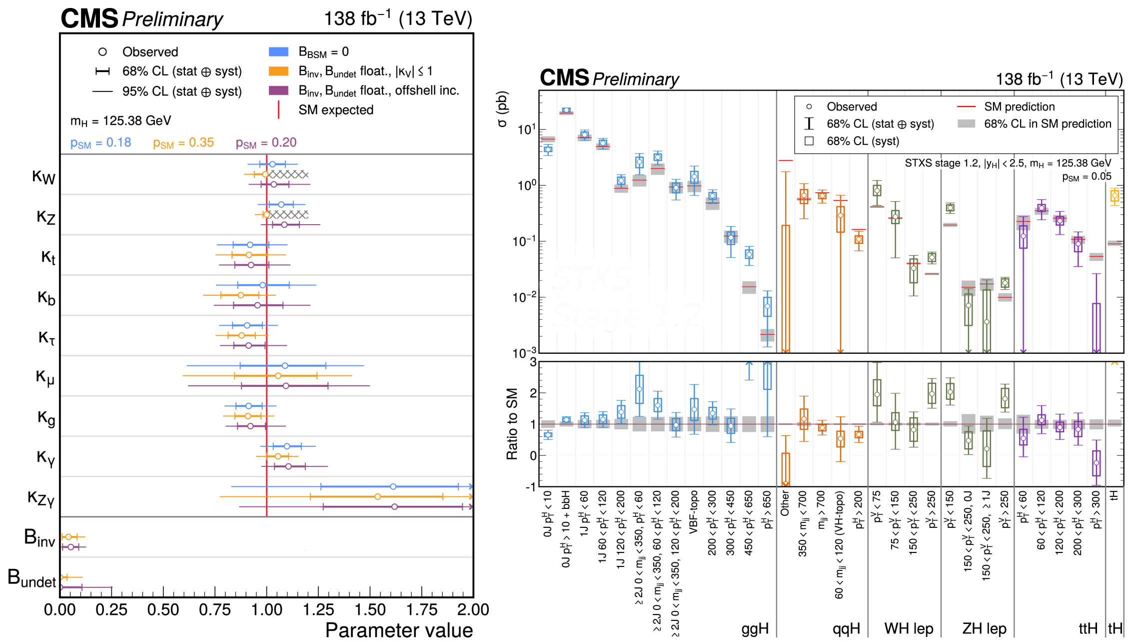

Figure 5: Selection of combined results from CMS interpreted in (left) the so-called κ-framework and (right) the stage 1.2 of the STXS framework [15].

with Standard Model expectations, though the overall precision remains limited by data statistics. A significance of 4.7σ is reported in this channel on inclusive $t\bar{t}H$ production versus the null hypothesis.

In the $t\bar{t}H(H \to bb)$ channel, ATLAS reported a signal strength of $\mu_{t\bar{t}H} = 0.81^{+0.20}_{-0.18}$ with a significance of 4.7σ [19], while the most precise CMS measurement obtained $\mu_{t\bar{t}H} = 0.91^{+0.26}_{-0.18}$ with 4.4σ [20]. Both measurements are dominated by systematic uncertainties and agree with the Standard Model. An improved background model as well as a better optimised selection allowed to improve significantly the signal-to-background ratio in the ATLAS measurement (see Figure 6) with respect to the previous ATLAS publication [21], while CMS achieved an impressive sensitivity in the full hadronic channel due to a very high rejection of the QCD background. CMS also set limits on tH production and constrained the CP structure of the top–Higgs interaction in a previous publication [22]. Finally, CMS has carried out the first search for $t\bar{t}H(H \to cc)$, performed simultaneously with a measurement of inclusive $t\bar{t}H \to bb$ production [20]. This search yielded the most stringent limit to date on the charm Yukawa coupling modifier, $|\kappa_c| < 3.5$, when combined with VH results (see Figure 7).

6. Higgs–b/c sector (Run 2)

ATLAS released a extensive combined study of $VH(H \to bb/cc)$ [23], including 0ℓ, 1ℓ and 2ℓ channels as well as a boosted $H \to b\bar{b}$ channel. The measured signal strength is $\mu^{bb}_{VH} = 0.92^{+0.16}_{-0.14}$, reaching a significance of 7.4σ. The analysis is also used to set a 300%-improved limit with respect to the last iteration on the Higgs coupling to charm quarks, $|\kappa_c| < 4.2$ (see Figure 8).

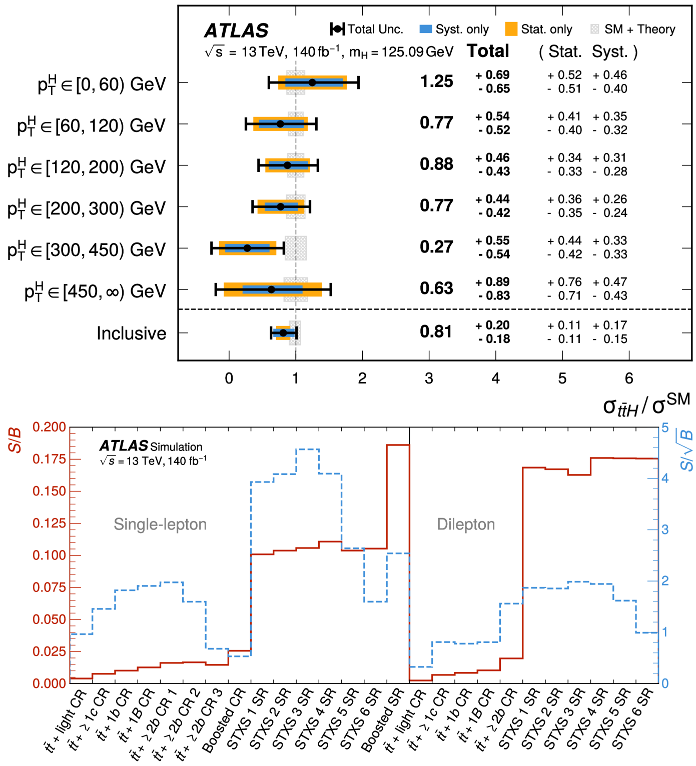

Figure 6: (top) ATLAS $t\bar{t}H(H \to b\bar{b})$ measurement interpreted in the STXS framework and (bottom) signal-to-background ratio (S/B) and signal-to-square root of the background ratio (S/$\sqrt{B}$) in the various regions defined in the ATLAS $t\bar{t}H(H \to b\bar{b})$ analysis [19].

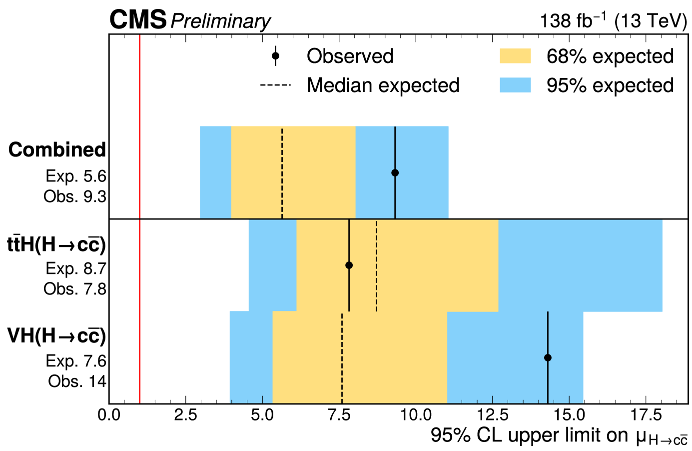

Figure 7: 95% CL upper limits on the $H \to c\bar{c}$ signal strength reported by CMS [20].

CMS recently reported the most precise boosted $V(qq)H$ search [24] at high p_T using advanced jet tagging (see Figure 9), where a significance of 1σ is reached on VH production, as well as an EFT interpretation of a revisited $VH(bb)$ analysis based on boosted information trees and including angular observables [25].

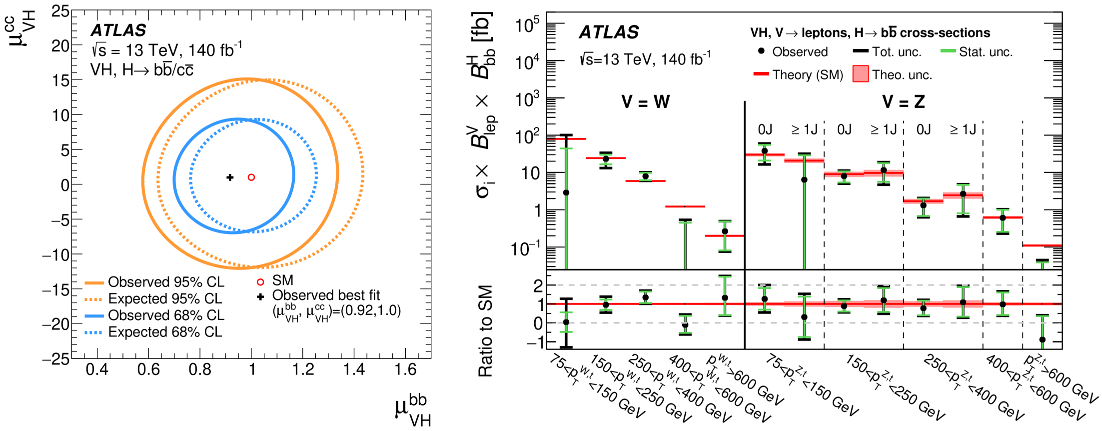

Figure 8: 2D profile likelihood projection on the $VH(H \to bb/cc)$ signal strengths and interpretation of the $VH(H \to bb/cc)$ measurements in the extended simplified template cross-section framework as reported by ATLAS [23].

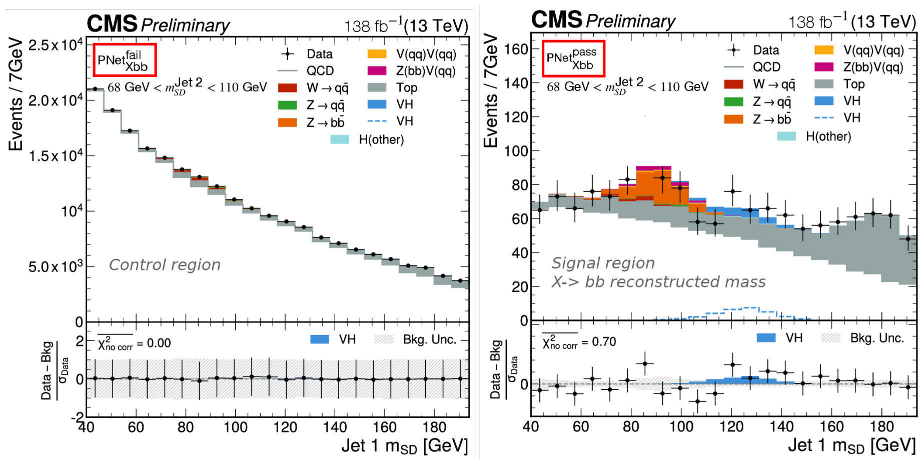

Figure 9: Distribution of the boosted Higgs boson candidate mass in (left) the top background control region and (right) the signal region, as reported by CMS in the $V(qq)H$ search [24].

7. Higgs–W/Z sector (Run 2)

The bosonic decay modes of the Higgs boson also provide a rich testing ground for precision studies and searches for new physics. ATLAS has measured $H \to WW^*$ decays in VH [26] as well as in gluon-gluon fusion (ggF) and vector-boson fusion (VBF) production [27], extracting both inclusive and differential cross sections. The ggF+VBF analysis includes measurements in STXS-like categories and provides an interpretation in terms of EFT operators, including CP-violating structures (see Figure 10). Complementary results from CMS [28] target $H \to WW^*$ production in association with two jets, focusing on the azimuthal separation of the jets, $\Delta\phi_{jj}$. The analysis employs adversarial deep neural networks for unfolding and constrains both CP-even and CP-odd SMEFT operators (see Figure 11). ATLAS has also extended its STXS analysis of $WH(H \to bb)$ to probe CP properties through angular observables [29], setting competitive limits on the related CP-odd operator ($H\tilde{W} \in [-0.62, 0.85]$ at 95% CL vs $H\tilde{W} \in [-1.0, 0.6]$ at 95% CL in the VBF analysis). In addition, CMS reported the first searches for boosted $H \to WW^*$ decays [30] and for associated $cH(H \to WW^*)$ production [31]. The latter is used to set a limit on the charm Yukawa coupling modifier, $|\kappa_c| < 211$ at the 95% CL (versus $|\kappa_c| < 38.1$ from $cH(H \to \gamma\gamma)$ [32] and $|\kappa_c| < 3.5$ from the combined ttH and VH analyses described in Section 5). While still limited by statistics, these studies demonstrate the feasibility of probing Higgs couplings in novel topologies.

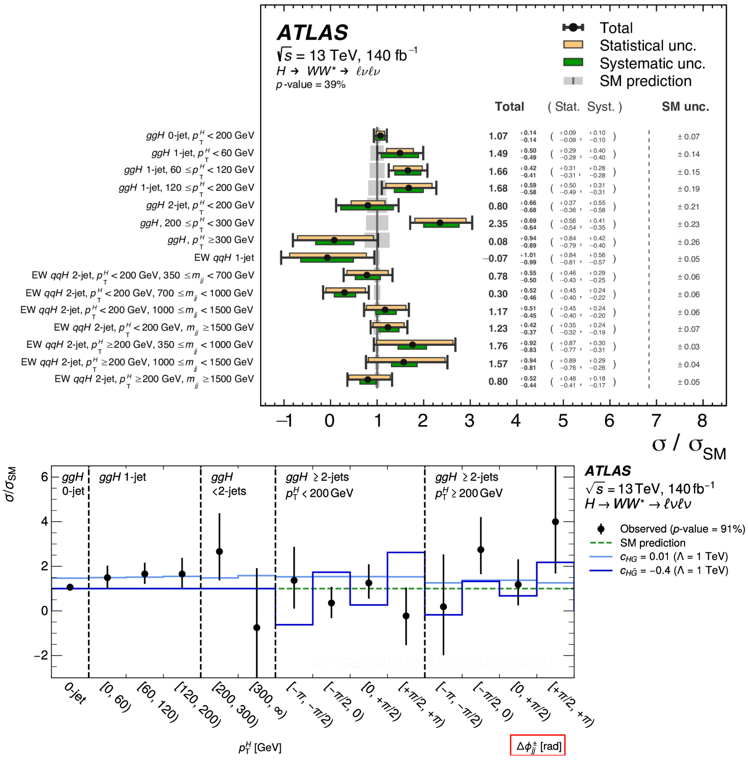

Figure 10: (top) ggF+VBF $H \to WW^*$ ATLAS measurement interpreted in the STXS framework. (bottom) STXS-like $\Delta\phi_{jj}$ measurement in the ggF+VBF $H \to WW^*$ channel interpreted with CP-violating EFT operators [27].

8. Summary and outlook

ATLAS and CMS have produced an extensive set of precision Run 2 measurements on the Higgs boson and its couplings, achieving substantial improvements in precision and sensitivity. Early Run 3 results confirm excellent detector performance and so far consistency with the SM. With the Run 3 dataset expected to double the Run 2 statistics, many new measurements will follow. Looking further ahead, the high luminosity LHC will provide an order-of-magnitude larger dataset, allowing unprecedented precision and detailed exploration of the Higgs sector.

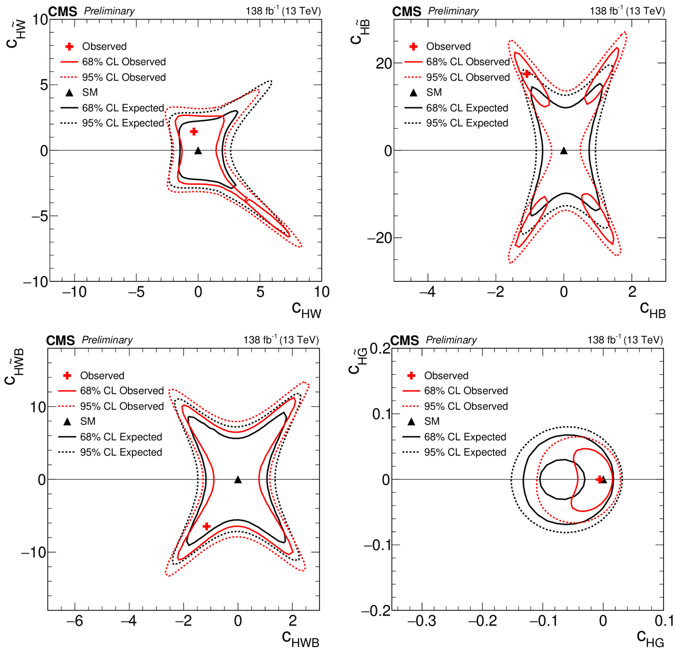

Figure 11: 2D profile likelihood scans for various pairs of Wilson coefficients from the CMS $H \to WW^* +$ 2 jets analysis [28]. CP-odd operators include a tilde symbol while CP-even operators do not. Solid (dotted) lines correspond to the 68% CL (95% CL) contours.

References

[1] ATLAS Collaboration, JINST **3** (2008), S08003.

[2] CMS Collaboration, JINST **3** (2008), S08004.

[3] CMS Collaboration, “CMS Public Luminosity Results,” https://twiki.cern.ch/twiki/bin/view/CMSPublic/LumiPublicResults#Summary_charts_of_luminosity.

[4] ATLAS Collaboration, Eur. Phys. J. C **85** (2025) 606.

[5] ATLAS Collaboration, ATLAS-CONF-2025-002, CERN, Geneva, 2025.

[6] CMS Collaboration, JHEP **05** (2025), 079.

[7] ATLAS Collaboration, Eur. Phys. J. C **84** (2024) 78.

[8] CMS Collaboration, CMS-PAS-HIG-23-014, CERN, Geneva, 2024.

[9] ATLAS Collaboration, Rept. Prog. Phys. **88** (2025) 057803.

[10] CMS Collaboration, Phys. Rev. D **111** (2025) 092014.

[11] ATLAS Collaboration, arXiv:2504.07710 [hep-ex].

[12] ATLAS Collaboration, Phys. Lett. B **847** (2023), 138315.

[13] ATLAS Collaboration, Phys. Rev. Lett. **131** (2023) 251802.

[14] CMS Collaboration, Phys. Lett. B **805** (2020), 135425.

[15] CMS Collaboration, CMS-PAS-HIG-21-018, CERN, Geneva, 2025.

[16] N. Berger *et al.*, arXiv:1906.02754 [hep-ph], LHCHXSWG-2019-003, DESY-19-070 (2019).

[17] ATLAS Collaboration, Nature **607** (2022) no.7917, 52-59 [erratum: Nature **612** (2022) no.7941, E24].

[18] CMS Collaboration, CMS-PAS-HIG-23-015, CERN, Geneva, 2025.

[19] ATLAS Collaboration, Eur. Phys. J. C **85** (2025) 210.

[20] CMS Collaboration, arXiv:2509.22535 [hep-ex].

[21] ATLAS Collaboration, JHEP **06** (2022), 097

[22] CMS Collaboration, JHEP **02** (2025), 097.

[23] ATLAS Collaboration, JHEP **04** (2025), 075.

[24] CMS Collaboration, CMS-PAS-HIG-24-017, CERN, Geneva, 2025.

[25] CMS Collaboration, JHEP **03** (2025), 114.

[26] ATLAS Collaboration, JHEP **08** (2025), 034.

[27] ATLAS Collaboration, arXiv:2504.07686 [hep-ex].

[28] CMS Collaboration, CMS-PAS-HIG-24-004 , CERN, Geneva, 2024.

[29] ATLAS Collaboration, ATL-PHYS-PUB-2025-022, CERN, Geneva, 2025.

[30] CMS Collaboration, CMS-PAS-HIG-24-008, CERN, Geneva, 2025.

[31] CMS Collaboration, arXiv:2508.14988 [hep-ex].

[32] CMS Collaboration, arXiv:2503.08797 [hep-ex].

PoS(LHCP2025)134